Analytica Chimica Acta 1045 (2019) 132–140

Contents lists available at ScienceDirect

Analytica Chimica Acta

journal homepage: www.elsevier.com/locate/aca

Magnetic ionic liquid-enhanced isothermal nucleic acid amplification and its application to rapid visual DNA analysis

Xiong Ding, Kevin D. Clark, Marcelino Varona, Miranda N. Emaus, Jared L. Anderson*

Department of Chemistry, Iowa State University, Ames, IA, 50011, USA

HIGHLIGHTS

- Magnetic ionic liquid-compatible isothermal nucleic acid amplification (MIL-INAA) was developed.
- MIL-INAA significantly reduced the background fluorescence in real-time detection.
- MIL-INAA accelerated target-loaded amplification with a shorter threshold time.
- Closed-tube visual detection of MIL-INAA product was established.
- Rapid visual DNA analysis from cell lysates was achieved using MIL-INAA and MILbased DNA extraction.

GRAPHICAL ABSTRACT

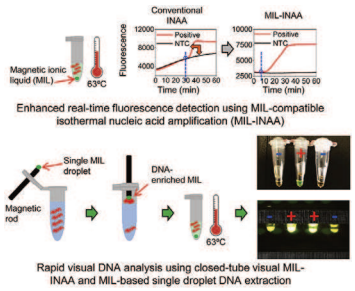

ARTICLE INFO

Article history:
Received 6 July 2018
Received in revised form
3 September 2018
Accepted 8 September 2018
Available online 12 September 2018

Keywords:
Isothermal nucleic acid amplification
Magnetic ionic liquid
Real-time fluorescence detection
Visual detection of product
Rapid visual DNA analysis

ABSTRACT

Isothermal nucleic acid amplification (INAA) techniques such as loop-mediated isothermal amplification (LAMP) and isothermal multiple-self-matching-initiated amplification (IMSA) constitute simple and rapid approaches for the detection of pathogens. However, due to the employment of multiple primers, the detection of LAMP and IMSA products is easily influenced by high background signals from primer dimer-based nonspecific nucleic acid amplification (NSA) products. Moreover, time-consuming sample preparation steps are often required for the isolation of sufficiently pure nucleic acid prior to INAA. To address these drawbacks, hydrophobic magnetic ionic liquids (MILs) were used to rapidly preconcentrate DNA from complex biological samples followed by direct amplification by LAMP and IMSA. Careful control of the components within the isothermal buffer permitted direct addition of DNA-enriched MIL to the INAA reaction mixture, thereby circumventing tedious purification procedures that are ordinarily required prior to downstream DNA amplification. When added directly to INAA reactions, MIL solvents released metal ions that ultimately inhibited the primer dimer-mediated NSA, resulting in a flat or decreased baseline signal in no-template control samples and short threshold time for positive reactions. Using a MIL-based single droplet DNA extraction method, MIL-enhanced INAA reaction system, and a handheld 3D printed device for visual detection of the amplified product in customized tubes, we demonstrate the potential of the MIL-based approach for the onsite analysis of DNA from pathogens.

1. Introduction

Isothermal nucleic acid amplification (INAA) is an alternative to standard amplification methods such as polymerase chain reaction

* Corresponding author. Department of Chemistry, 1605 Gilman Hall, Iowa State University, Ames, IA, 50011, USA.
E-mail address: andersoj@iastate.edu (J.L. Anderson).

https://doi.org/10.1016/j.aca.2018.09.014
0003-2670/

(PCR) for the rapid detection of nucleic acids from pathogens. Notable advantages of INAA include speed, high sensitivity, high specificity, and independence from thermal cyclers [1]. INAA techniques such as loop-mediated isothermal amplification (LAMP) and isothermal multiple-self-matching-initiated amplification (IMSA) are promising for onsite detection applications as their signal output can be detected visually or in real-time with a portable fluorescence measuring instrument [2–6].

A major limitation of LAMP and IMSA for onsite applications is the high background fluorescence caused by nonspecific amplification (NSA) resulting from carryover contamination and primer dimer formation. The increased background fluorescence from NSA interferes with the fluorescence signal produced by target DNA amplification, ultimately delaying the threshold time (Tt) for positive reactions and making it more difficult to distinguish between a positive reaction and no-template control. The Tt to exponential fluorescence curve is defined similarly as the Cq value in qPCR. Carryover contamination can lead to false positive results as the fluorescence curve obtained is identical to one produced by positive amplification [7]. Carryover contamination can be avoided by using closed-tube reactions, a restriction endonuclease, or by addition of the uracil-DNA glycosylase to digest pre-embedded uracil in contaminating amplification products [8–10]. Since LAMP and IMSA require the use of multiple primers for target amplification, the likelihood of primer dimer-based NSA is increased and results in a higher fluorescence baseline for real-time detection using a double-stranded DNA (dsDNA) intercalating dye such as SYBR Green I (SG) [11]. Dual-labeled strand exchange or displacement probes can also be used for improving detection specificity, but these specialty oligonucleotides are expensive and require complicated probe design [12,13]. Unfortunately, the only cost-efficient strategy to eliminate primer dimer-based NSA is the repeated design, evaluation, and optimization of multiple primer sets. However, even when optimized primers that minimize NSA are employed, primers can still form duplexes in the reaction mixture and result in high background signal from dsDNA intercalating dyes.

To obtain purified nucleic acids, commercial extraction kits employing silica-based membranes are commonly used in LAMP and IMSA [14–17]. However, these kits require multiple tedious centrifugation or vacuum-assisted steps to separate and purify nucleic acids from interferences in a process that involves cumbersome equipment that is unsuitable for onsite detection. To overcome these limitations, magnetic ionic liquid (MIL) solvents have been applied for rapid nucleic acid purification. MILs are molten salts exhibiting paramagnetic behavior with physicochemical properties that can be tuned for specific applications by modifying the cation and anion structure [18]. The potential mechanism of MIL capturing DNA may involve a combination of electrostatic and $\pi-\pi$ interactions between DNA and the structures of cations or anions [19,20]. The nucleic acid enriched MIL droplet can be easily manipulated with an external magnetic field to quickly remove the solvent from biological samples [20,21].

In this study, MIL-compatible LAMP and IMSA (MIL-LAMP and MIL-IMSA) reaction systems were developed and evaluated in order to seamlessly integrate MIL-based sample preparation with INAA for rapid, onsite DNA analysis. We designed new isothermal buffer systems in order to relieve the inhibitory effects of two hydrophobic MILs on INAA. Unexpectedly, the optimized MIL-containing reaction system diminished primer dimer-based NSA by decreasing the melting temperature (T_m) of dsDNA fragments in the isothermal amplification buffer. As a result, MIL-enhanced real-time LAMP and IMSA were successfully achieved with lower baseline signals as determined by real-time fluorescence measurements. Compared to standard real-time LAMP and IMSA, MIL-LAMP and MIL-IMSA provided accelerated positive amplification with the Tt as short as 30 min for the amplification of 405 copies target DNA molecules. In addition, visual detection of the MIL-IMSA product was achieved using a closed tube system and a handheld 3D printed device, demonstrating the feasibility of the MIL-based approach for onsite visual DNA analysis. By coupling MIL-based single drop DNA extraction to visual MIL-IMSA, we achieved rapid DNA detection from a complex biological sample (10^3 CFU mL^{-1} *Escherichia Coli* cells with target plasmid) in less than 35 min.

2. Experimental section

2.1. Materials

Trihexyl(tetradecyl)phosphonium chloride (over 93%) was purchased from Strem Chemicals (Newburyport, MA, USA). Ethylene glycol tetraacetic acid (EGTA), nickel(II) chloride hexahydrate, and cobalt(II) chloride hexahydrate were purchased from Sigma Aldrich (St. Louis, MO, USA). Two hydrophobic MILs with low viscosity recently invented by our group were used in this study, the trihexyl(tetradecyl)phosphonium tris(hexafluoroacetylaceto)nickelate(II) ($[P^+_{66614}][Ni(II)(hfacac)^-_3]$) and trihexyl(tetradecyl)phosphonium tris(hexafluoroacetylaceto)cobaltate(II) ($[P^+_{66614}][Co(II)(hfacac)^-_3]$). The $[P^+_{66614}][Ni(II)(hfacac)^-_3]$ and $[P^+_{66614}][Co(II)(hfacac)^-_3]$ MILs were synthesized and characterized according to the procedures previously reported by our group [22]. Their chemical structures are shown in Fig. 1A.

The 10 mM dNTPs, 8000 U mL^{-1} *Bst* 2.0 WarmStart DNA polymerase, 100 mM Mg_2SO_4, and 10 × Isothermal Amplification Buffer (200 mM Tris-HCl, 500 mM KCl, 100 mM $(NH_4)_2SO_4$, 20 mM $MgSO_4$, 1% Tween-20, pH 8.8 at 25 °C) were obtained from New England BioLabs (Ipswich, MA, USA). Nuclease-free water and 10000 × SG were purchased from Thermo Fisher Scientific (Waltham, MA, USA). The 5 M betaine was obtained from Sigma-Aldrich (St. Louis, MO, USA). Ultra-pure water (18.2 MΩ cm) was obtained using a Milli-Q water purification system (Millipore, Bedford, MA, USA). The pCR 2.1 plasmid (3.9 kb) inserted with a 280 bp fragment of S-protein gene from HBV genome was provided by Eurofins Genomics (Louisville, KY, USA). All primers were synthesized by Integrated DNA Technologies (Coralville, IA, USA).

2.2. Standard LAMP and IMSA assays

The amplification principles of LAMP and IMSA are described in Fig. S1. The standard LAMP reaction system was composed of 1 × Isothermal Amplification Buffer, 6 mM $MgSO_4$, 1.4 mM dNTPs, 0.2 μM each of outer primers (F3 and B3), 1.6 μM each of inner primers (FIP and BIP), 0.8 μM each of loop primers (LF and LB), 3.2 U *Bst* 2.0 WarmStart DNA polymerase, 0.8 M betaine, 1 × SG dye, and 1.0 μL of template DNA solution or 1.0 μL nuclease-free water to replace target DNA as a no-template control (NTC). The standard IMSA reaction system was the same as standard LAMP. The target DNA sequence for both LAMP and IMSA was a 280 bp fragment of the S-protein gene from hepatitis B virus (HBV) inserted into a plasmid. Sequence information for corresponding primers and targets are shown in Table S1. The total volume of reaction solution was 10 μL. The reactions were incubated at 63 °C for 60 min in a Bio-Rad CFX Connect Real-Time PCR Detection System (Hercules, CA, USA) for real-time fluorescence detection.

2.3. Visual MIL-IMSA assay

Closed-tube visual detection of amplification products was developed using the optimal $[P^+_{66614}][Ni(II)(hfacac)^-_3]$ MIL-IMSA. The visual MIL-IMSA assay was conducted in a PCR tube that also held a

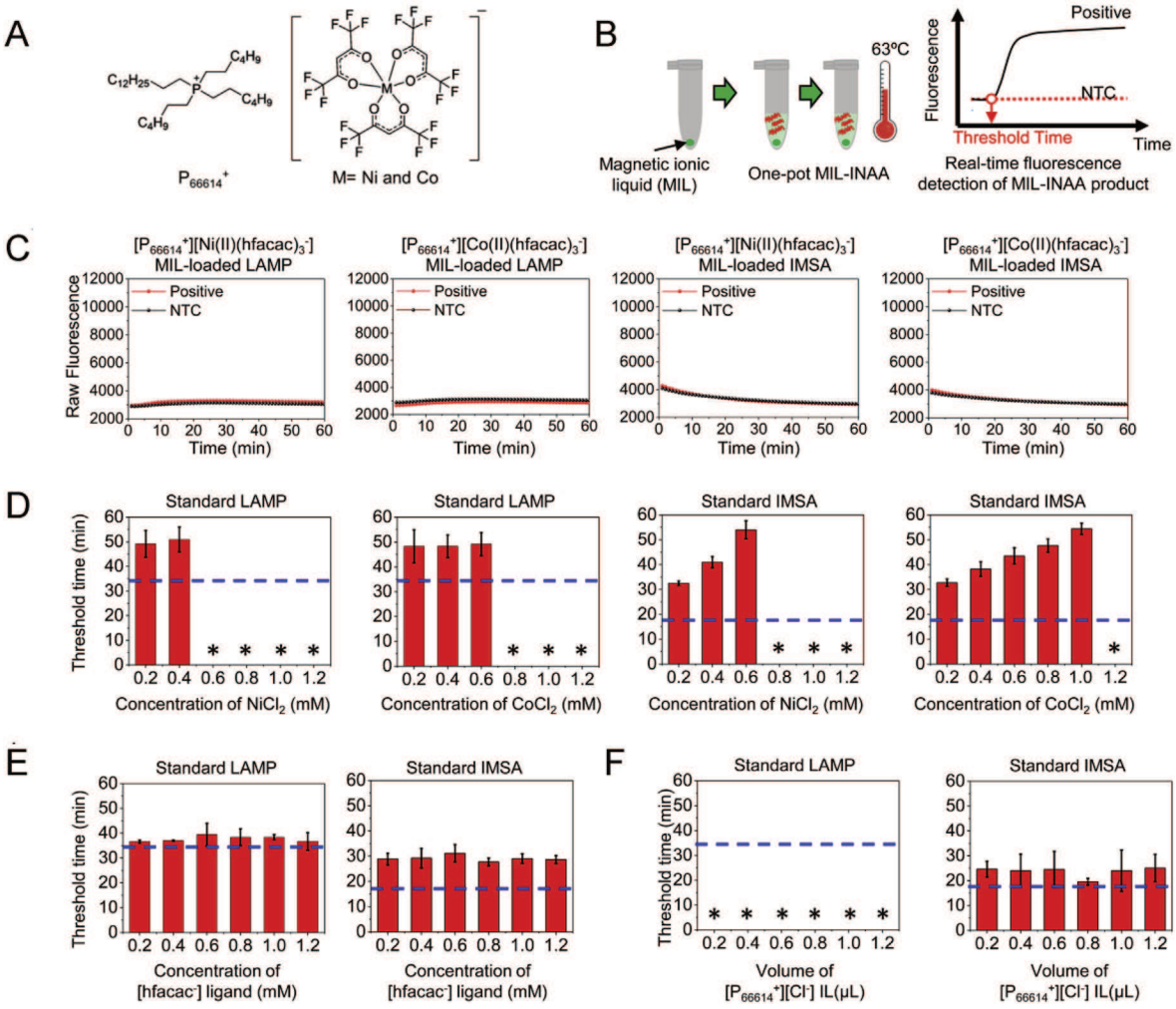

Fig. 1. (A) Structures of the two hydrophobic MILs examined in this study. (B) Workflow of the MIL compatibility assays using real-time fluorescence detection of INAA. (C) Real-time fluorescence change for standard LAMP and IMSA directly added with $[P^{+}_{66614}][Ni(II)(hfacac)^{-}_{3}]$ or $[P^{+}_{66614}][Co(II)(hfacac)^{-}_{3}]$ MIL. The volume of MIL was 0.5 μL. (D–F) Effect of various amounts of Ni^{2+} (added as $NiCl_2$), Co^{2+} (as $CoCl_2$), [hfacac$^-$] (as 1,1,1,5,5,5-hexafluoroacetylacetone), and $[P^{+}_{66614}]$ (as the $[P^{+}_{66614}][Cl^-]$ ionic liquid (IL)) on standard LAMP and IMSA. Horizontal dashed blue lines represented the threshold time of standard positive LAMP and IMSA reactions. Positive, reactions with 6.33×10^6 copies of target DNA. NTC, no-template control. Each error bar represents the standard deviation for three tests. * Not detected within the 60-min reaction time. (For interpretation of the references to color in this figure legend, the reader is referred to the Web version of this article.)

small secondary container filled with 1000 × SG in order to separate the dye from the reaction solution. Prior to inserting the container, the MIL-IMSA reaction system was added. The reaction system was similar to that of optimal MIL-IMSA, only excluding the SG dye. The template solutions were prepared by 5-fold serial dilution to yield concentrations ranging from 8.10×10^1 to 1.27×10^6 copies per reaction. After incubation at 63 °C for 45 min in a simple incubator (e.g., water bath), the color change of the reaction solution was observed under a black background after inverting and shaking the tubes for several times to mix the 1000 × SG with the amplicon.

2.4. Cell culture and the preparation of cell lysate

Competent *E. coli* K12 cells were transformed with the pCR 2.1 plasmid encoding S-protein gene fragment from HBV. Approximately 25 ng of purified plasmid DNA was added to a microcentrifuge tube containing 10 μL of NEB 5-alpha Competent *E. coli* cells and gently mixed. The solution was placed on ice for 30 min then set in a water bath at 42 °C for 42 s. Immediately afterward, the cells were chilled on ice for 5 min. After transforming the cells, 950 μL of Luria Bertani (LB) media was added to the solution and incubated at 37 °C for 1 h. The *E. coli* cells were subsequently transferred into 2 mL of LB media with 100 μg mL^{-1} carbenicillin at 37 °C for 24 h. A 170 μL aliquot of LB media with 10^4, 10^3, or 10^2 CFU mL^{-1} cells was lysed using 250 μL Buffer P1 containing LyseBlue reagent from the QIAGEN QIAprep Spin Miniprep Kit. Following the lysis protocol, the volume was brought up to 2 mL with deionized water prior to the MIL-based single droplet extraction (SDE).

2.5. Onsite visual detection coupled with MIL-based single droplet DNA extraction

The procedure for the MIL-based SDE method was performed as shown in Fig. S3. Briefly, a small magnetic rod ($B = 0.20$ T; D1X0, K&J Magnetics, Inc.) was first inserted through the lid of a 2.0-mL plastic centrifuge tube. A 2.0 μL droplet of MIL was placed on the magnet then directly immersed into a 2 mL cell lysate solution containing target DNA and subjected to shaking at 250 rpm for

5 min in an incubation shaker for DNA extraction. The rod was then carefully removed to avoid contact with the lid. Following the extraction, 0.5 μL of DNA-enriched MIL was subjected to closed-tube visual MIL-IMSA as previously described. After incubation at 63 °C for 30 min in a water bath, the color change of the reaction solution under a black background was observed after thoroughly inverting the tubes several times. In addition, a handheld device was fabricated using an Ultimaker 3D Printer (Geldermalsen, The Netherlands) to enable fluorescence-based onsite visual detection. ABS filament (2.85 mm) was obtained from MatterHackers, Chicago, IL, USA. The device was designed using a 3D graphics software provided by 3D Universe. Following the MIL-IMSA reaction, a high-contrast fluorescence change was observed between NTC and positive reaction solutions.

3. Results and discussion

3.1. The development of MIL-INAA

The ideal MIL-INAA reaction system should seamlessly integrate the MIL within the isothermal reaction buffer. Therefore, the effects of the $[P^{+}_{66614}][Ni(II)(hfacac)^{-}_{3}]$ and $[P^{+}_{66614}][Co(II)(hfacac)^{-}_{3}]$ MILs in the LAMP and IMSA reaction systems were investigated. LAMP and IMSA reactions containing 0.5 μL MIL and target DNA were performed using real-time fluorescence detection (see Fig. 1B). As shown in Fig. 1C, the amplification curves for the positive LAMP and IMSA reactions were indistinguishable from the NTC, indicating that the examined MILs inhibited LAMP and IMSA and could not be directly added to the INAA reaction mix without the customization of the buffer.

Although the MILs examined in this study were highly hydrophobic, small amounts of the $[P^{+}_{66614}][Ni(II)(hfacac)^{-}_{3}]$ or $[P^{+}_{66614}][Co(II)(hfacac)^{-}_{3}]$ MIL solvent may dissolve in aqueous solution at elevated temperature [22]. Accordingly, we hypothesized that the inhibition was likely caused by the release of one or more structural components of the MIL (metal ions, $[hfacac^{-}]$ ligand, and $[P^{+}_{66614}]$ cation) into the reaction mixture. To test this hypothesis, we investigated the effect of the various MIL structural components on standard LAMP and IMSA reactions. As shown in Fig. 1D–F, the addition of the MIL structural components generally resulted in longer Tt for both LAMP and IMSA reactions. Fig. 1D shows that the minimum inhibitory concentrations (MICs) for Ni^{2+} and Co^{2+} in standard LAMP were 0.6 mM and 0.8 mM, respectively. In contrast, IMSA exhibited a higher tolerance as the MICs of Ni^{2+} and Co^{2+} reached 0.8 mM and 1.2 mM, respectively. In reactions containing $[hfacac^{-}]$ ligand, Fig. 1E shows that up to 1.2 mM $[hfacac^{-}]$ could be tolerated by both LAMP and IMSA. When the $[P^{+}_{66614}][Cl^{-}]$ IL was investigated, considerable inhibition of LAMP was observed even when 0.2 μL of the IL was added to the reaction (see Fig. 1F). In contrast, IMSA could tolerate up to 1.2 μL of the IL. The results above suggest that the inhibition of LAMP and IMSA caused by the MILs originated from the metal ions and/or the $[P^{+}_{66614}]$ cation released from the MIL. According to previous reports, the divalent metal ions Ni^{2+} and Co^{2+} can distort the geometry of the DNA polymerase active site resulting in either a decrease in synthesis fidelity or total reaction inhibition [23,24]. Thus, it is plausible that the released Ni^{2+} and Co^{2+} ions can decrease the activity of *Bst* DNA polymerase.

To determine the amount of Ni^{2+} released from the $[P^{+}_{66614}][Ni(II)(hfacac)^{-}_{3}]$ MIL into the aqueous phase of the IMSA standard reaction as a representation, flame atomic absorption spectroscopy assays were conducted. As shown in Fig. S4, approximately 8.4 mM Ni^{2+} was released from the MIL into the aqueous solution after incubation at 63 °C for 60 min. This concentration is much greater than the previously determined MIC of Ni^{2+} (0.6 mM), further supporting the hypothesis that inhibition is likely due to the release of metal ions from the MIL into the aqueous reaction mixture.

In order to couple the nucleic acid extraction capabilities of MILs with LAMP and IMSA for rapid DNA analysis, the inhibitory effects of MILs must be overcome. Metal ion chelators such as EGTA or EDTA are commonly used as additives to relieve inhibition caused by metal ions in PCR [25,26]. Therefore, the addition of various EGTA concentrations to MIL-containing LAMP and IMSA reaction systems was studied. As shown in Fig. 2A, amplification was successfully recovered for MIL-LAMP and MIL-IMSA by using 5 mM EGTA as an additive. In addition, relieving the inhibitory effects of MILs results from the interaction between EGTA and MIL rather than the interaction between EGTA and isothermal amplification buffer, since Fig. S5 shows that the standard reactions with EGTA are obviously inhibited and the addition of EGTA into MIL can relieve inhibition originating from the dissolved MIL. As demonstrated above, both the metal ions and the $[P^{+}_{66614}]$ cation can cause inhibition in LAMP. However, amplification in MIL-loaded LAMP was recovered by using EGTA, suggesting that the metal ions released by the MIL played a larger role in the amplification inhibition of LAMP.

3.2. Mechanism of MIL-mediated inhibition of primer dimer-based NSA in INAA

When developing real-time INAA, a major concern is the appearance of positive amplification signals for NTC samples due to primer dimer-based NSA or carryover contamination. As shown in Fig. 2A, primer dimer-based NSA in standard LAMP and IMSA can produce strong background signals in real-time fluorescence detection. Compared to the NTC in standard INAA, Fig. 2A shows that the primer dimer-based NSA in MIL-INAA NTC was inhibited, since there was no accumulated dsDNA to slowly raise the baseline.

Interestingly, Fig. 2A also shows that the NTC in MIL-IMSA showed a gradual decrease in the change of fluorescence. Since a dsDNA structure (i.e., primer dimer) is formed by the FIT and RIT IMSA primers (see Table S1), the gradual decrease in baseline fluorescence may be attributed to the interaction between the dissolved MIL and the dsDNA structure. To test this, the fluorescence intensity change of the solution containing the mixture of FIT and RIT was investigated when a 2.0 μL aliquot of aqueous phase from the co-incubation (63 °C for 60 min) of MIL (0.5 μL) and SG (2 ×) water solution was tested. As shown in Fig. 2B, a significant decrease in fluorescence intensity was observed.

The effect of metal ions on DNA hybridization has previously been investigated [27]. In order to determine whether the MILs or the metal ions influence the annealing of the primers to the target DNA, the T_m of a model 20 bp duplex DNA (a fragment obtained from the S-protein gene; see Table S1) in the isothermal amplification buffer was investigated. As shown in Fig. 2C, a lower T_m was observed for the duplex DNA in the presence of the $[P^{+}_{66614}][Ni(II)(hfacac)^{-}_{3}]$ or $[P^{+}_{66614}][Co(II)(hfacac)^{-}_{3}]$ MIL. The effect of various MIL structural components (Ni^{2+}, Co^{2+}, $[hfacac^{-}]$ ligand, and $[P^{+}_{66614}]$ cation) on the T_m of the same duplex DNA was also investigated. Fig. S6A shows that increasing concentrations of Ni^{2+} and Co^{2+} resulted in an obvious decrease in the T_m. However, the T_m was not affected by $[hfacac^{-}]$ or the $[P^{+}_{66614}][Cl^{-}]$ IL. Similar results were achieved by using the same duplex DNA sequence but labeled with a fluorophore and quencher (see Fig. S6B). These data support a mechanism in which the released metal ions from the MIL can decrease the T_m of the double-stranded DNA (dsDNA) target, which probably enhances the annealing of primers to the dsDNA target in INAA. Although higher metal ion concentrations result in reaction inhibition, the addition of EGTA helps mitigate this effect and allow a small amount of free metal ions to increase INAA reaction speed.

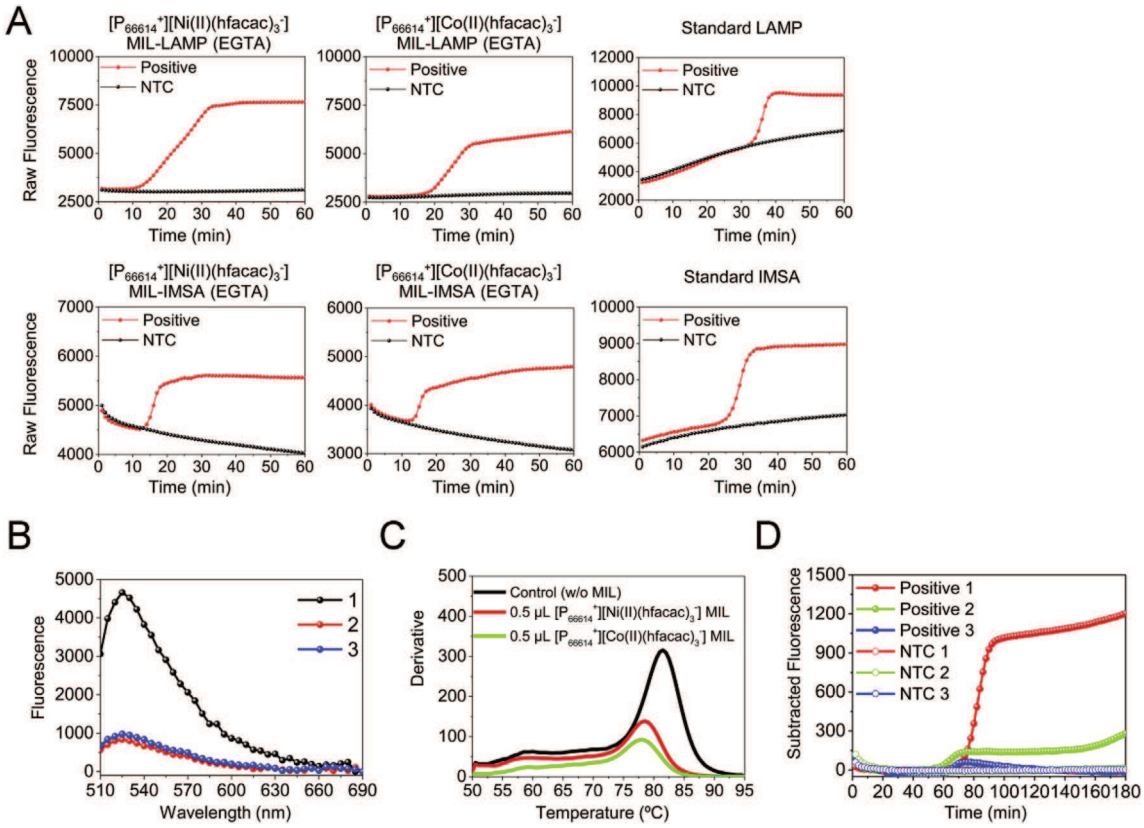

Fig. 2. (A) Real-time fluorescence change in MIL-LAMP and MIL-IMSA with 5 mM EGTA, and the standard LAMP and IMSA reactions. (B) Fluorescence spectrum of a DNA solution (0.5 μM primer mixture of FIT and RIT from IMSA) with the 2.0 μL aliquot of aqueous phase (AP) from the MIL and SG (2 ×) after being co-incubated at 63 °C for 60 min. 1–3: test without any AP but with SG, test with AP from $[P^{+}_{66614}][Ni(II)(hfacac)^{-}_{3}]$ MIL and SG, and test with AP from $[P^{+}_{66614}][Co(II)(hfacac)^{-}_{3}]$ MIL and SG. (C) Melt curve derivative result of a duplex DNA (1 μM Duplex 1 in Table S1) in 1 × isothermal amplification buffer including 8 mM $MgSO_4$ with and without MIL. The volume of MIL was 0.5 μL. (D) Real-time fluorescence change in MIL-loaded UIMA with 5 mM EGTA. 1–3: UIMA without any MIL, UIMA with $[P^{+}_{66614}][Ni(II)(hfacac)^{-}_{3}]$ MIL, and UIMA with $[P^{+}_{66614}][Co(II)(hfacac)^{-}_{3}]$ MIL. Positive for LAMP and IMSA, the reaction with 6.33×10^6 copies of target DNA. Positive for UIMA, the reaction with 10 nM ssDNA template. NTC, no-template control. Subtracted fluorescence is the background subtracted fluorescence.

To study whether the MIL could inhibit primer dimer-based NSA, we added the MILs into the unusual isothermal multimerization and amplification (UIMA) reaction (Figure S2), a typical primer dimer-based NSA that complicate the products of LAMP and IMSA [28]. As shown in Fig. 2D, UIMA was significantly inhibited when supplemented with 0.5 μL of $[P^{+}_{66614}][Ni(II)(hfacac)^{-}_{3}]$ or $[P^{+}_{66614}][Co(II)(hfacac)^{-}_{3}]$ MIL. These experiments show that the addition of MILs in INAA can inhibit primer dimer-NSA. This significant reduction in primer dimer-based NSA could reduce the occurrence of false positives in INAA's endpoint detection, which is very important for onsite diagnostics.

3.3. Metal ions and the $[P^{+}_{66614}]$ cation decrease fluorescence intensity in MIL-INAA

When compared to standard reactions, both MIL-LAMP and MIL-IMSA showed decreased fluorescence intensity for both positive and no-template control (NTC) reactions (see Fig. 2A). Fig. 2B shows that the MIL could affect the fluorescence of the dsDNA-SG complex. In order to determine the cause of the diminished fluorescence, fluorescence spectra of the INAA reaction system (excluding the primers and target DNA) were collected at room temperature after being supplemented with various amounts of MIL structural components and a controlled amount of duplex DNA. As shown in Fig. S7, the addition of both metal ions (Ni^{2+} and Co^{2+}) and the $[P^{+}_{66614}][Cl^{-}]$ IL cation resulted in noticeably lower fluorescence intensity. However, the $[P^{+}_{66614}][Cl^{-}]$ IL produced the largest decrease in fluorescence signal. The reduced fluorescence caused by adding metal ions to the reaction system may result from the destabilization of dsDNA (vide supra). However, since no observable change in T_m was caused by the addition of $[P^{+}_{66614}][Cl^{-}]$ IL, the decrease in fluorescence intensity is likely due to the partitioning of SG dye to the hydrophobic IL [29]. Thus, the decrease in fluorescence intensity observed in MIL-INAA is most likely due to a combination of the effects from the released metal ions and the $[P^{+}_{66614}]$ cation. Nevertheless, the amplification curves in positive MIL-INAA reactions still retain the characteristic exponential amplification shape that is identical to the standards.

3.4. Optimal MIL-INAA and comparison with optimal standard INAA

In an attempt to achieve lower Tt for rapid DNA analysis, MIL-LAMP and MIL-IMSA were optimized in the same way as standard reaction systems, by varying the amounts of EGTA, MIL, $MgSO_4$, dNTPs, and betaine while monitoring the Tt in real-time. The results of optimization assays are displayed in Table S5. The sensitivities of optimal MIL-LAMP and MIL-IMSA reactions were then evaluated by assaying a range of target plasmid DNA concentrations. Fig. 3A shows that $[P^{+}_{66614}][Co(II)(hfacac)^{-}_{3}]$ MIL-LAMP achieved lower Tt and a lower detection limit (4.05×10^2 copies per reaction) than $[P^{+}_{66614}][Ni(II)(hfacac)^{-}_{3}]$ MIL-LAMP (2.03×10^3 copies per reaction). On the other hand, the Tt was higher for $[P^{+}_{66614}][Co(II)(hfacac)^{-}_{3}]$ MIL-IMSA than $[P^{+}_{66614}][Ni(II)(hfacac)^{-}_{3}]$ MIL-IMSA,

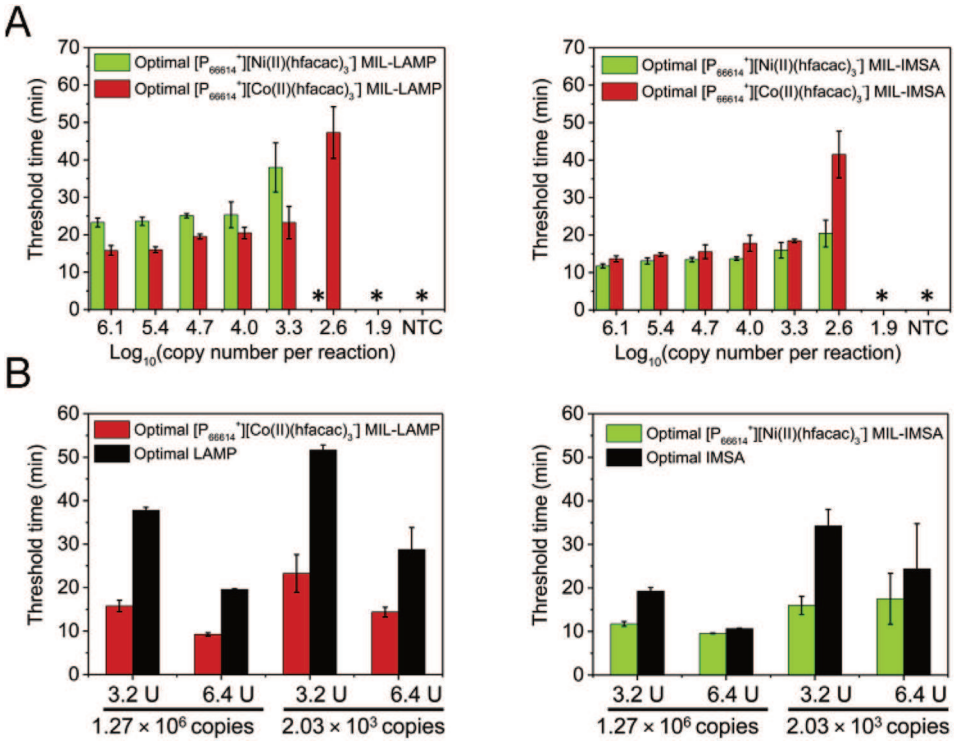

Fig. 3. (A) Threshold time for optimal MIL-LAMP and MIL-IMSA with various copies of target DNA. (B) Comparison assay of optimal MIL-INAA ($[P^{+}_{66614}][Co(II)(hfacac)^{-}_{3}]$ MIL-LAMP and $[P^{+}_{66614}][Ni(II)(hfacac)^{-}_{3}]$ MIL-IMSA) and optimal conventional LAMP and IMSA on threshold time of positive reactions using different units (U) of *Bst* DNA polymerase. Each error bar represents the standard deviation for three technical tests. NTC, no-template control.* Not detected within the 60-min reaction time.

despite having the same detection limit (4.05×10^2 copies per reaction). Next, the Tt for the optimized MIL-INAA systems ($[P^{+}_{66614}][Co(II)(hfacac)^{-}_{3}]$ MIL-LAMP and $[P^{+}_{66614}][Ni(II)(hfacac)^{-}_{3}]$ MIL-IMSA) was compared with the Tt of the optimized standard INAA (see Table S5). As shown in Fig. 3B, the Tt for MIL-INAA was shorter than standard INAA, even when the amount of *Bst* DNA polymerase was increased to 6.4 U per reaction. Moreover, the Tt in both MIL-LAMP and MIL-IMSA with 3.2 U Bst was shorter than standard INAA using 6.4 U for the amplification of 2.03×10^3 copies target DNA. Since *Bst* DNA polymerase is the most expensive component of the buffer, MIL-INAA represents a cost-efficient alternative to enable rapid nucleic acid amplification.

3.5. Closed-tube visual MIL-IMSA

In order to demonstrate the feasibility for onsite DNA analysis, visual detection of the MIL-INAA product was developed using the optimal $[P^{+}_{66614}][Ni(II)(hfacac)^{-}_{3}]$ MIL-IMSA reaction in a closed tube or a handheld 3D printed device using hydroxynaphthol blue (HNB). HNB is often used for closed-tube visual LAMP and IMSA because it is compatible with the reaction system and can be added prior to amplification [15,30,31]. After amplification, the color of HNB-loaded solution changes from purple to sky blue, due to the consumption of magnesium ion (Mg^{2+}) during the reaction. Unfortunately, there was a strong precipitation-like interaction between MIL and HNB dye (see Fig. S8). When supplementing the HNB-loaded IMSA reaction mixture with MIL, Fig. S8 shows that a light red color was maintained after amplification. Thus, HNB can't be used to realize visual MIL-IMSA.

Therefore, SG was considered as a replacement of HNB. However, to achieve visual detection of the product, a relatively high concentration of SG dye (e.g., 1000 × SG) was required. This concentration of SG strongly inhibits the MIL-IMSA if added prior to the amplification step [32,33]. To overcome this inhibition of amplification, microcrystalline wax with a melting point at 85 °C has previously been used to encapsulate the SG dye [32,33]. However, heating the solidified wax to release the dye into the amplified products requires a heat source capable of generating high enough temperatures to melt the wax, rendering this method incompatible for field-testing applications. Instead, a small customized container was made to separate 1000 × SG dye from the MIL-IMSA reaction solution to prevent the inhibition caused by excess SG in the reaction solution. As shown in Fig. 4A, the customized container was prepared by cutting a PCR tube and subsequently applying pressure to make an eye-like orifice that enables the efficient mixing of dye and the amplified products. In order to prevent the container from coming into contact with the reaction solution while maintaining some movability, the optimal container size was calculated to be approximately 5 mm in diameter (D) and 6 mm in height (H) (see Fig. S9). Following amplification, the reaction tubes can be inverted multiple times to allow the SG dye in the container to mix with the reaction solution. After the dye and reaction solution are well mixed, a clear color change can be observed for all positive reactions that can easily be differentiated from the NTC (see Fig. 4B). Using the optimized $[P^{+}_{66614}][Ni(II)(hfacac)^{-}_{3}]$ MIL-IMSA reaction system, the sensitivity using the aforementioned visual detection method was also investigated. As shown in Fig. 4B, a green color was observed following amplification of various concentrations of target DNA. The results indicate that this method can be used to visually detect down to 4.06×10^2 copies of target DNA, showing the same sensitivity as real-time detection. Therefore, the developed visual MIL-INAA holds great promise for onsite applications as no sophisticated instrument is required for the detection of amplification products.

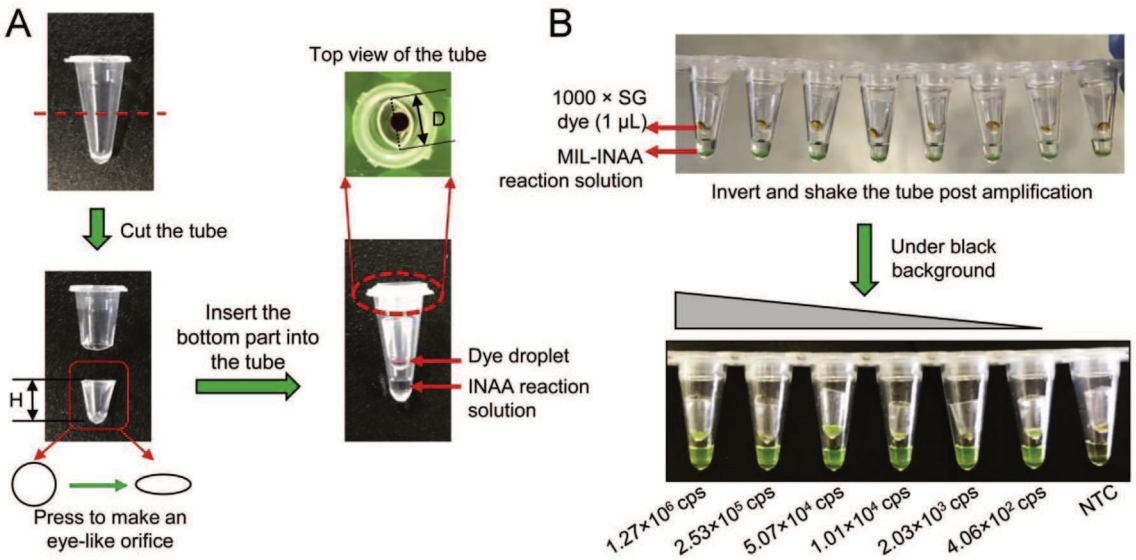

Fig. 4. Close-tube visual MIL-INAA. (A) Schematic illustrating the process for the fabrication of small customized container. For easy presentation, the hydroxynaphthol blue dye of 480 μM was used a model. D and H, the diameter and height of the container. (B) Appearance of the closed tube for visual MIL-INAA and the sensitivity of the visual $[P^{+}_{66614}][Ni(II)(hfacac)_3]$ MIL-IMSA for the detection of various amounts of S-protein gene fragment-contained plasmid DNA. Cps, copies per reaction. NTC, the no-template control. (For interpretation of the references to color in this figure legend, the reader is referred to the Web version of this article.)

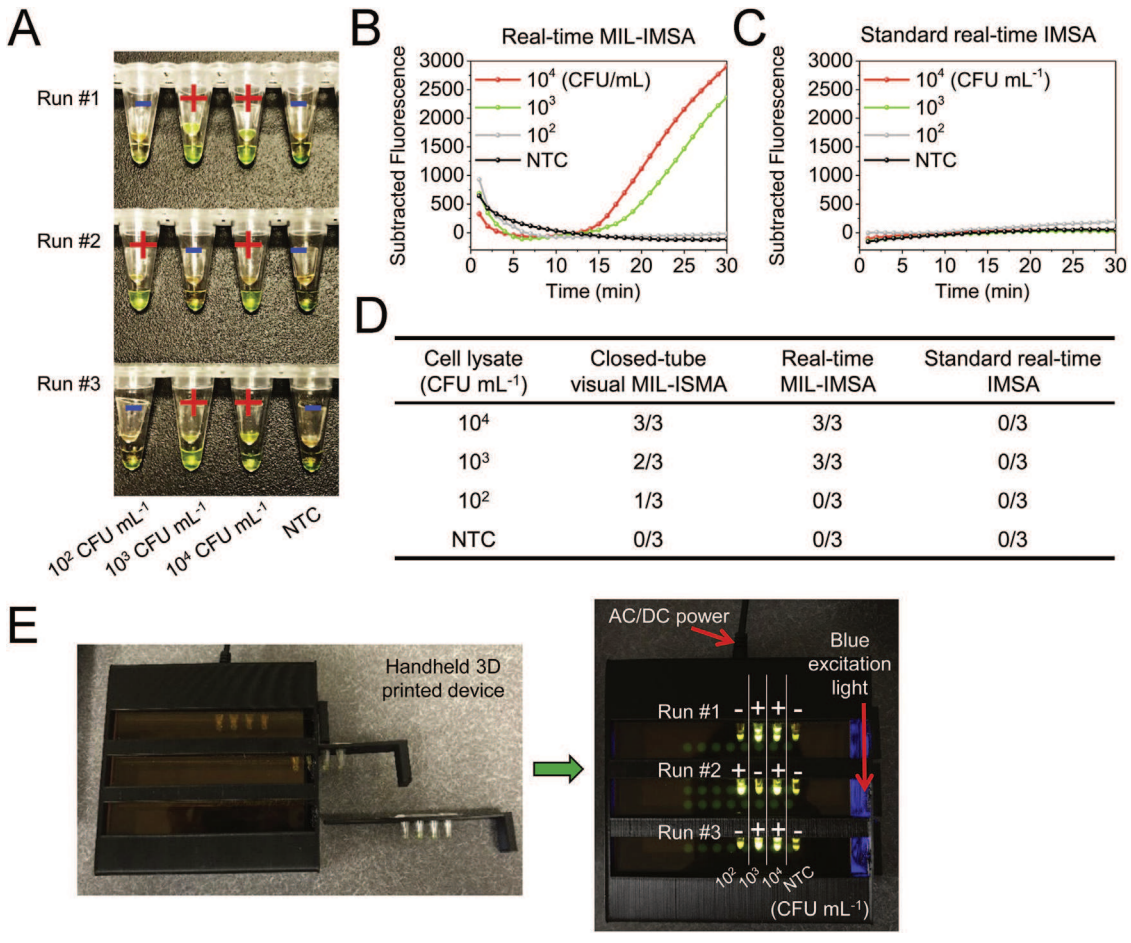

Cell lysate (CFU mL^{-1})	Closed-tube visual MIL-ISMA	Real-time MIL-IMSA	Standard real-time IMSA
10^4	3/3	3/3	0/3
10^3	2/3	3/3	0/3
10^2	1/3	0/3	0/3
NTC	0/3	0/3	0/3

Fig. 5. Real-time and visual DNA analysis from cell lysates with various amounts. (A) Closed-tube visual MIL-IMSA following the MIL-based single droplet DNA extraction (SDE). (B) Real-time MIL-IMSA following the MIL-based SDE. (C) Standard real-time IMSA using directly added 1 μL of cell lysate as the template. (D) The table indicating the ratio of number of positive result to total number of test when running the three experimental replicate tests for closed-tube MIL-IMSA, real-time MIL-IMSA, and standard real-time IMSA. (E) Fluorescence-based visual detection of MIL-IMSA product using a handheld 3D printed device following the MIL-based SDE. Enlarged photo to illustrate the fluorescence-based visual detection result is shown in Fig. S11. Positive (+), the reaction with target DNA. NTC (−), the no-template control.

3.6. MIL-based single-drop extraction enables rapid onsite visual DNA analysis from cell lysate

In order to determine the feasibility of the method for onsite visual DNA detection, MIL-IMSA was directly interfaced with MIL-based SDE for the analysis of DNA from bacterial cell lysate. The schematic of optimized MIL-based SDE is shown in Fig. S3. Prior to MIL extraction, *E. coli* cells transformed with a plasmid containing the target DNA insert were subjected to alkaline lysis. After the lysis step, a 5 min SDE was performed using 2 μL of MIL. Following the extraction step, a 0.5 μL aliquot of DNA-enriched MIL was transferred to a PCR tube containing the optimized MIL-INAA buffer. As shown in Fig. 5A, visual MIL-IMSA could detect DNA from cell suspensions containing 10^4 and 10^3 CFU mL^{-1} with 100% and 66.7% identification rate of positive (percentage of positive test number out of total test number) in 30 min, respectively. Therefore, by coupling MIL-based SDE to visual MIL-IMSA, we could achieve rapid visual DNA analysis from a complex biological sample (the lysate of 10^3 CFU mL^{-1} cells) in less than 35 min.

On detection sensitivity, Fig. 5B and D shows that closed-tube visual MIL-IMSA was comparable to real-time MIL-IMSA in the large fluorescence instrument. Moreover, Fig. 5A and D shows that visual MIL-IMSA had a change (33.3% identification rate) to identify DNA from the lysate of 10^2 CFU mL^{-1} cells. However, standard real-time IMSA was entirely inhibited when directly adding a 1.0 μL aliquot of the cell lysate as the template (see Fig. 5C and D). Thus, MIL-based SDE is beneficial for preconcentration of sufficiently pure target DNA devoid of the inhibitors present in the cell lysate.

To further facilitate onsite fluorescence detection of the MIL-IMSA amplification products, a 3D printed handheld device was designed. As shown in Fig. S10, the device (115 mm × 115 mm × 55 mm) consists of two major elements: a blue LED light array to generate the excitation light at a wavelength of 450 nm and an orange glass filter to remove background wavelengths below 470 nm. Two plug-in holders and three tube fixation holders were added in order to hold sample tubes. After the incubation step, the tubes can be placed inside the sliding strip, inserted into the device, and exposed to blue excitation light generated by a AC/DC power converter (12 V and 6 A). Fig. 5E shows that a strong green fluorescence was clearly produced in the positive reactions and the detection sensitivity was the same as that of closed-tube visual MIL-IMSA. By replacing the AC/DC converter with a portable battery or power bank, this device can easily be used for onsite DNA analysis of pathogens.

4. Conclusions

In this study, MILs were successfully interfaced with LAMP and IMSA reaction systems by using EGTA as an additive to relieve inhibition of amplification. MIL-LAMP and MIL-IMSA can accelerate amplification and inhibit primer dimer-based nonspecific amplification for real-time detection. Furthermore, they can be used for visual detection using closed tubes and a handheld 3D printed device. Rapid visual DNA analysis from cell lysate (10^4 and 10^3 CFU mL^{-1} cell lysate) can be achieved in as short as 35 min. Therefore, we conclude that the developed MIL-enhanced INAA reaction systems holds great promise for pathogen diagnostics, particularly in onsite applications.

Declarations of interest

The authors declare no competing financial interest.

Acknowledgements

JLA acknowledges support from the Chemical Measurement and Imaging Program at the National Science Foundation (Grant no. CHE-1709372).

Appendix A. Supplementary data

Supplementary data to this article can be found online at https://doi.org/10.1016/j.aca.2018.09.014.

References

[1] Y. Zhao, F. Chen, Q. Li, L. Wang, C. Fan, Isothermal amplification of nucleic acids, Chem. Rev. 115 (2015) 12491–12545.
[2] X. Ding, W. Wu, Q. Zhu, T. Zhang, W. Jin, Y. Mu, Mixed-dye-based label-free and sensitive dual fluorescence for the product detection of nucleic acid isothermal multiple-self-matching-initiated amplification, Anal. Chem. 87 (2015) 10306–10314.
[3] M. Yi, L. Ling, S.B. Neogi, Y. Fan, D. Tang, S. Yamasaki, L. Shi, L. Ye, Real time loop-mediated isothermal amplification using a portable fluorescence scanner for rapid and simple detection of Vibrio parahaemolyticus, Food Contr. 41 (2014) 91–95.
[4] X. Ding, K. Nie, L. Shi, Y. Zhang, L. Guan, D. Zhang, S. Qi, X. Ma, Improved detection limit in rapid detection of human enterovirus 71 and coxsackievirus A16 by a novel reverse transcription–isothermal multiple-self-matching-initiated amplification assay, J. Clin. Microbiol. 52 (2014) 1862–1870.
[5] N. Tomita, Y. Mori, H. Kanda, T. Notomi, Loop-mediated isothermal amplification (LAMP) of gene sequences and simple visual detection of products, Nat. Protoc. 3 (2008) 877–882.
[6] C. Escadafal, O. Faye, O. Faye, M. Weidmann, O. Strohmeier, F. von Stetten, J. Drexler, M. Eberhard, M. Niedrig, P. Patel, Rapid molecular assays for the detection of yellow fever virus in low-resource settings, PLoS Neglected Trop. Dis. 8 (2014), https://doi.org/10.1371/journal.pntd.0002730.
[7] K. Hsieh, P.L. Mage, A.T. Csordas, M. Eisenstein, H.T. Soh, Simultaneous elimination of carryover contamination and detection of DNA with uracil-DNA-glycosylase-supplemented loop-mediated isothermal amplification (UDG-LAMP), Chem. Commun. (J. Chem. Soc. Sect. D) 50 (2014) 3747–3749.
[8] Y. Wang, D. Liu, J. Deng, Y. Wang, J. Xu, C. Ye, Loop-mediated isothermal amplification using self-avoiding molecular recognition systems and antarctic thermal sensitive uracil-DNA-glycosylase for detection of nucleic acid with prevention of carryover contamination, Anal. Chim. Acta 996 (2017) 74–87.
[9] C.K. Nkere, J.O. Oyekanmi, G. Silva, M. Bömer, G.I. Atiri, J. Onyeka, N.G. Maroya, S.E. Seal, P.L. Kumar, Chromogenic detection of yam mosaic virus by closed-tube reverse transcription loop-mediated isothermal amplification (CT-RT-LAMP), Arch. Virol. (2018) 1–5.
[10] C. Ma, F. Wang, X. Wang, L. Han, H. Jing, H. Zhang, C. Shi, A novel method to control carryover contamination in isothermal nucleic acid amplification, Chem. Commun. (J. Chem. Soc. Sect. D) 53 (2017) 10696–10699.
[11] J. Peng, Y. Zhan, F. Zeng, H. Long, Y. Pei, J. Guo, Development of a real-time fluorescence loop-mediated isothermal amplification assay for rapid and quantitative detection of Fusarium oxysporum f. sp. niveum in soil, FEMS Microbiol. Lett. 349 (2013) 127–134.
[12] Y.S. Jiang, S. Bhadra, B. Li, Y.R. Wu, J.N. Milligan, A.D. Ellington, Robust strand exchange reactions for the sequence-specific, real-time detection of nucleic acid amplicons, Anal. Chem. 87 (2015) 3314–3320.
[13] X. Ding, G. Wang, J. Sun, T. Zhang, Y. Mu, Fluorogenic bidirectional displacement probe-based real-time isothermal DNA amplification and specific visual detection of products, Chem. Commun. (J. Chem. Soc. Sect. D) 52 (2016) 11438–11441.
[14] L. Luo, K. Nie, M.-J. Yang, M. Wang, J. Li, C. Zhang, H.-T. Liu, X.-J. Ma, Visual detection of high-risk human papillomavirus genotypes 16, 18, 45, 52, and 58 by loop-mediated isothermal amplification with hydroxynaphthol blue dye, J. Clin. Microbiol. 49 (2011) 3545–3550.
[15] J. Luo, Z. Xu, K. Nie, X. Ding, L. Guan, J. Wang, Y. Xian, X. Wu, X. Ma, Visual detection of norovirus genogroup II by reverse transcription loop-mediated isothermal amplification with hydroxynaphthol blue dye, Food Environ. Virol. 6 (2014) 196–201.
[16] S. Günther, S. Felten, G. Wess, K. Hartmann, K. Weber, Detection of feline Coronavirus in effusions of cats with and without feline infectious peritonitis using loop-mediated isothermal amplification, J. Virol. Methods 256 (2018) 32–36.
[17] S.A. Besuschio, M.L. Murcia, A.F. Benatar, S. Monnerat, I. Cruz, A. Picado, M. de los Ángeles Curto, Y. Kubota, D.P. Wehrendt, P. Pavia, Analytical sensitivity and specificity of a loop-mediated isothermal amplification (LAMP) kit prototype for detection of Trypanosoma cruzi DNA in human blood samples, PLoS Neglected Trop. Dis. 11 (2017), https://doi.org/10.1371/journal.pntd.0005779.
[18] M. Li, S.L. De Rooy, D.K. Bwambok, B. El-Zahab, J.F. DiTusa, I.M. Warner, Magnetic chiral ionic liquids derived from amino acids, Chem. Commun. (J. Chem. Soc. Sect. D) (2009) 6922–6924.
[19] T. Li, M.D. Joshi, D.R. Ronning, J.L. Anderson, Ionic liquids as solvents for in situ dispersive liquid–liquid microextraction of DNA, J. Chromatogr. A 1272 (2013) 8–14.
[20] K.D. Clark, O. Nacham, H. Yu, T. Li, M.M. Yamsek, D.R. Ronning, J.L. Anderson, Extraction of DNA by magnetic ionic liquids: tunable solvents for rapid and

selective DNA analysis, Anal. Chem. 87 (2015) 1552–1559.
[21] K.D. Clark, M.M. Yamsek, O. Nacham, J.L. Anderson, Magnetic ionic liquids as PCR-compatible solvents for DNA extraction from biological samples, Chem. Commun. (J. Chem. Soc. Sect. D) 51 (2015) 16771–16773.
[22] S.A. Pierson, O. Nacham, K.D. Clark, H. Nan, Y. Mudryk, J.L. Anderson, Synthesis and characterization of low viscosity hexafluoroacetylacetonate-based hydrophobic magnetic ionic liquids, New J. Chem. 41 (2017) 5498–5505.
[23] H. Pelletier, M.R. Sawaya, W. Wolfle, S.H. Wilson, J. Kraut, A structural basis for metal ion mutagenicity and nucleotide selectivity in human DNA polymerase β, Biochemistry 35 (1996) 12762–12777.
[24] M.A. Sirover, L.A. Loeb, Infidelity of DNA synthesis in vitro: screening for potential metal mutagens or carcinogens, Science 194 (1976) 1434–1436.
[25] J. Bickley, D. Hopkins, Inhibitors and enhancers of PCR, in: Analytical Molecular Biology: Quality and Validation, 1999, pp. 81–102.
[26] L. Rossen, P. Nørskov, K. Holmstrøm, O.F. Rasmussen, Inhibition of PCR by components of food samples, microbial diagnostic assays and DNA-extraction solutions, Int. J. Food Microbiol. 17 (1992) 37–45.
[27] J.G. Duguid, V.A. Bloomfield, J.M. Benevides, G.J. Thomas Jr., Raman spectroscopy of DNA-metal complexes. II. The thermal denaturation of DNA in the presence of Sr2+, Ba2+, Mg2+, Ca2+, Mn2+, Co2+, Ni2+, and Cd2+, Biophys. J. 69 (1995) 2623–2641.
[28] G. Wang, X. Ding, J. Hu, W. Wu, J. Sun, Y. Mu, Unusual isothermal multimerization and amplification by the strand-displacing DNA polymerases with reverse transcription activities, Sci. Rep. 7 (2017) 13928.
[29] P.-J. JimmyáHuang, Extraction of DNA staining dyes from DNA using hydrophobic ionic liquids, Chem. Commun. (J. Chem. Soc. Sect. D) 49 (2013) 4537–4539.
[30] D. Liu, B. Zhao, X. Ou, H. Zheng, A. Ma, W. He, S. Wang, Y. Zhou, H. Xia, Y. Zheng, A novel isothermal amplification-based method to detect Mycobacterium tuberculosis complex, J. Microbiol. Meth. 145 (2018) 59–65.
[31] X.-j. Ma, Y.-l. Shu, K. Nie, M. Qin, D.-y. Wang, R.-b. Gao, M. Wang, L.-y. Wen, F. Han, S.-m. Zhou, Visual detection of pandemic influenza A H1N1 Virus 2009 by reverse-transcription loop-mediated isothermal amplification with hydroxynaphthol blue dye, J. Virol. Methods 167 (2010) 214–217.
[32] M. Zhang, Y. Liu, L. Chen, S. Quan, S. Jiang, D. Zhang, L. Yang, One simple DNA extraction device and its combination with modified visual loop-mediated isothermal amplification for rapid on-field detection of genetically modified organisms, Anal. Chem. 85 (2012) 75–82.
[33] Z.-Y. Tao, H.-Y. Zhou, H. Xia, S. Xu, H.-W. Zhu, R.L. Culleton, E.-T. Han, F. Lu, Q. Fang, Y.-P. Gu, Adaptation of a visualized loop-mediated isothermal amplification technique for field detection of Plasmodium vivax infection, Parasites Vectors 4 (2011) 115.